ARTICLE Communicated by John Rinzel

Dynamics of Membrane Excitability Determine Interspike Interval Variability: A Link Between Spike Generation Mechanisms and Cortical Spike Train Statistics

Boris S. Gutkin
G. Bard Ermentrout
Program in Neurobiology and Department of Mathematics, University of Pittsburgh, Pittsburgh, PA 15260, U.S.A.

We propose a biophysical mechanism for the high interspike interval variability observed in cortical spike trains. The key lies in the nonlinear dynamics of cortical spike generation, which are consistent with type I membranes where saddle-node dynamics underlie excitability (Rinzel & Ermentrout, 1989). We present a canonical model for type I membranes, the θ-neuron. The θ-neuron is a phase model whose dynamics reflect salient features of type I membranes. This model generates spike trains with coefficient of variation (CV) above 0.6 when brought to firing by noisy inputs. This happens because the timing of spikes for a type I excitable cell is exquisitely sensitive to the amplitude of the suprathreshold stimulus pulses. A noisy input current, giving random amplitude "kicks" to the cell, evokes highly irregular firing across a wide range of firing rates; an intrinsically oscillating cell gives regular spike trains. We corroborate the results with simulations of the Morris-Lecar (M-L) neural model with random synaptic inputs: type I M-L yields high CVs. When this model is modified to have type II dynamics (periodicity arises via a Hopf bifurcation), however, it gives regular spike trains (CV below 0.3). Our results suggest that the high CV values such as those observed in cortical spike trains are an intrinsic characteristic of type I membranes driven to firing by "random" inputs. In contrast, neural oscillators or neurons exhibiting type II excitability should produce regular spike trains.

1 Introduction

The statistical nature of single neuron response has been a widely recognized feature of neural information processing. Historically, a number of preparations yielded spike trains with a large degree of variability (Burns & Webb, 1976; Kroner & Kaplan, 1993). Spike trains with high coefficients of variation (CV) have been reported for a wide range of stimulus-evoked activity of nonbursting pyramidal neurons in visual cortical areas of monkeys (Softky & Koch, 1993; Dean, 1981; McCormick, Connors, Lighthall, &

Prince, 1985). Such high in vivo interspike interval variability is contrasted with highly reproducible in vitro response of neurons to depolarizing current steps (Holt, Softky, Koch, & Douglas, 1996), aperiodic stimuli (Mainen & Sejnowski, 1995) and robust spike timing for high-contrast visual stimuli in vivo (Reich, Victor, Knight, Ozaki, & Kaplan, 1997). Softky and Koch (1993) presented an analysis of cortical spike trains, showing that neither the changes in the mean firing rate nor spike frequency adaptation could account for high CVs. To date, several hypotheses have been proposed to explain these seemingly paradoxical findings.

Classical stochastic models presented neurons as temporal integrators with spike generation as a random walk with an absorbing boundary (Stein, 1965; Ricciardi, 1994). Numerous variants of these random walk or stochastic integrate-and-fire (IF) models strove to account for nonstationary excitability of the neuron, nonlinear summation of the synaptic inputs, and multimodal output distributions (Smith, 1992; Wilbur & Rinzel, 1983).

Softky and Koch (1993) suggested that the high CVs are inconsistent with temporal integration of randomly arriving excitatory postsynaptic potentials (EPSPs). Based on studies of compartmental models with Hodgkin-Huxley spike-generating currents, they proposed that several mechanisms, most notably active dendritic processes, amplify weak temporal correlations in the input and produce highly variable input currents at the soma. The cell acts as a coincidence detector and produces noisy output.

An alternative hypothesis states that sufficiently variable input currents can be generated under a balance of excitatory and inhibitory inputs. The neuron then remains close to the threshold, and firing reflects the fine temporal fluctuations in the input current. Shadlen and Newsome (1994) found high CVs for the balanced Stein model and Bell, Mainen, Tsodyks, and Sejnowski (1995) found similar results for a Hodgkin-Huxley neuron under specific parameter choices. Networks with connectivity that ensures the excitatory-inhibitory balance also produce highly variable firing in noisy IF neurons (Usher, Stemmler, Koch, & Olami, 1994) and chaotic threshold elements (van Vreeswijk & Sompolinsky, 1996).

Recently Troyer and Miller (1997) showed that input-output properties of the neuron can strongly influence the integration of noisy inputs. They modified the leaky IF neuron to include a partial postspike reset voltage. Using the reset as a free parameter, they fitted IF neurons to real pyramidal in vitro response frequency to input current (FI) curves. They found that such IF neurons (termed "high gain")[1] give high CVs, and do so without a balance of inputs. Neurons where FI gain is much lower than seen in data did not produce high CVs. The explanation was that the "high-gain" IF neuron hovers near a steady state (set by the reset voltage) and remains sensitive to temporal fluctuations in the random inputs. The "low-gain" neuron spends

[1] Gain is defined as the slope of the FI curve.

much more time depolarizing toward the threshold and thus damps out the input variability.

The emphasis of previous studies (with the notable exception of Troyer & Miller, 1997) has been mainly on mechanisms that generate sufficiently variable input currents at the soma. By using either the simplest point neurons or a standard Hodgkin-Huxley soma, most of the authors referred to omitted from their analysis the nonlinear spike-generating dynamics and their role in spiking statistics.

In this article, we assume that the input at the soma is variable. Focusing on the nonlinear dynamics of spike-generating mechanism, we show how properties of neural membranes dominated by saddle-node dynamics (type I) yield firing statistics observed in in vivo recordings and in vitro input-output characteristics of cortical neurons. We argue that the key is the sensitive dependence of spike latency to the amplitude of the suprathreshold inputs evident in type I membranes.

We review the salient characteristics of type I membranes and contrast these with type II membranes. In section 3 we present the canonical model for type I membranes, the θ-neuron. We show that high CV spike trains arise for the θ-neuron in the excitable regime. The oscillating θ-neuron produces low CV firing patterns. We follow with an example of a more detailed spiking neural model (Morris-Lecar, M-L) in section 4. Simulations of type I Morris-Lecar corroborate our θ-neuron findings. Type II M-L yields low CV spike trains, suggesting that type II membranes do not produce highly variable spike trains.

2 Type I vs. Type II Neural Membrane Dynamics

Our major assumption is type I membrane excitability for the spike-generating soma. The general idea is to classify the cells by the dynamical structure that underlies the onset of autonomous periodic firing. A more complete discussion of this classification can be found in Rinzel and Ermentrout (1989). The classification, based on observations of squid axons, was proposed by Hodgkin (1948), who found arbitrarily low response frequencies and spike latencies for some axons (Type I) and a narrow range of responses with no spike delay for others (Type II). We use the M-L model to illustrate type I and type II characteristics.

Observationally, a type I membrane is recognized by a continuous FI curve that shows oscillations arising with arbitrarily low frequencies (see Figure 1a). It shows that the type I cell is capable of a wide range of firing frequencies and that near the threshold, the input-output gain is infinite. This suggests that in the excitable regime, a number of dynamical behaviors is possible depending on the strength of the time-dependent stimulus input. In Figure 1b we see that the spike latency for a type I neural model (here M-L) is strongly sensitive to the magnitude of the suprathreshold stimulus.

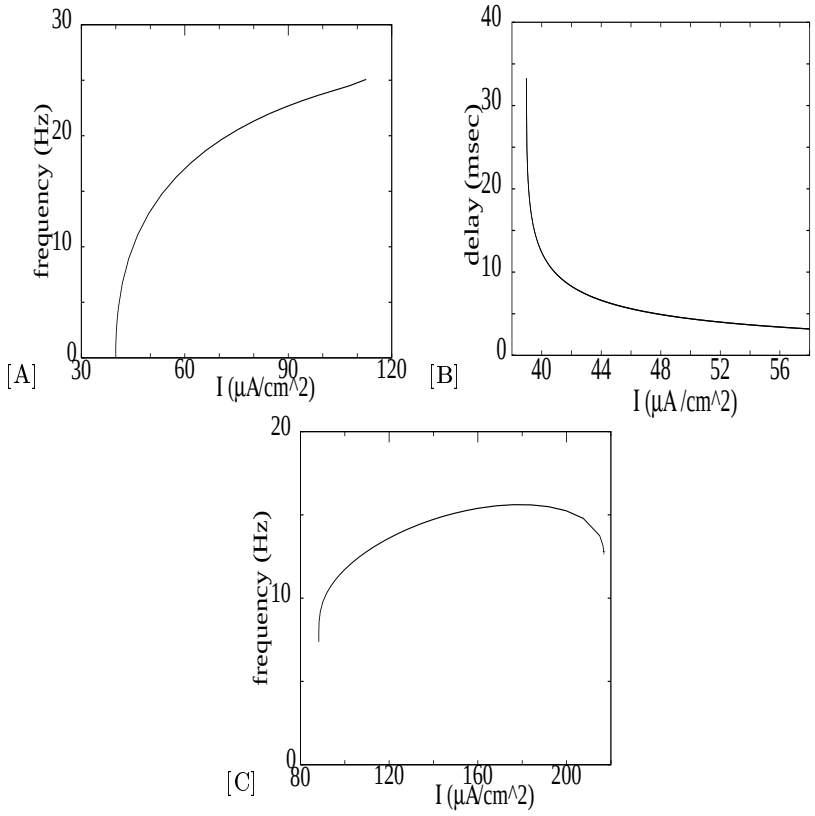

Figure 1: (a) Firing frequency to input current plot for type I membrane shows oscillations appearing with arbitrarily low frequencies. (b) The delay to spike in the type I model depends on the amplitude of the suprathreshold stimulus. (c) Firing frequency to input current plot for the type II shows oscillations arising with nonzero frequency.

Consider that temporal integration by the neural membrane acts to translate randomly timed synaptic inputs into a background DC bias (perhaps due to distant synapses) plus current with randomly varying amplitude (perhaps due to more proximal ones). Then a type I membrane, with its high spike latency sensitivity, converts the variability in the input current to variability in output spike timing. The phase plane for type I membrane helps us understand why this happens (see Figure 2a). The voltage nullcline intersects the activation nullcline, forming an attracting node and a saddle that acts as a threshold for the spike generation. A subthreshold stimulus would not evoke much response. Any stimulus pushing the voltage past

the saddle node will result in a spike of constant shape, but with a varying delay. This delay results from the fact that voltage trajectory near the threshold hugs the stable manifold of the saddle, moving rather slowly away from the threshold. Also, near the threshold, the membrane is most sensitive to small size inputs. As the voltage increases, the velocity of motion increases, and the membrane becomes insensitive to inputs because the active conductances dominate the dynamics. A fast spike is produced, followed by a refractory period and repolarization to the rest state. The important notion is the nonuniformity of motion around the phase plane. This is reminiscent of cortical neurons that, given a suprathreshold pulse stimulus, will slowly depolarize and then produce a fast spike.[2] We also note that a type I model spends most of its time near the steady state, just like the "high-gain" neuron of Troyer and Miller (1997).

We can change the excitability of the cell by increasing the bias current, which lifts the voltage nullcline. This lowers the threshold and reduces the region in the phase space where the membrane is most sensitive to input perturbations. With still more positive bias, the rest state disappears, and a limit cycle is left behind. This limit cycle is of constant amplitude but with a period dependent on the bias.

In contrast, type II membranes are characterized by discontinuous FI curves with the oscillations arising with a nonzero frequency. These oscillations are due to a subcritical Hopf bifurcation. The response frequency range is narrow and largely independent of the bias (see Figure 1c). There is also no true threshold for the appearance of spikes, which are not an all-or-nothing phenomenon, but with amplitude that can depend on the size of the pulse stimulus (see Figure 2c). The delay to spike is not sensitive to the size of the suprathreshold stimulus, and the long prespike depolarization is absent.

Several widely used cortical models are of type I—for example, Traub's model (Traub & Miles, 1991) and the Bower model (Wilson & Bower, 1989). Examples of type II membrane include the standard Hodgkin-Huxley model (Hodgkin & Huxley, 1952) and the FitzHugh-Nagumo reduced model (FitzHugh, 1961). The M-L model can be put into either the type I or the type II regime.

3 The θ-Neuron: A Canonical Model for Type I Membranes

We present a reduced neural phase model (θ-neuron) capable of reproducing spike-train statistics at a wide range of mean firing rates. The θ-neuron is a canonical model for type I membranes resulting from formal mathematical reduction of multidimensional neural models exhibiting type I dynamics. That is, every neural model with type I dynamics can be reduced to the

[2] This is thought to be due to the A-current.

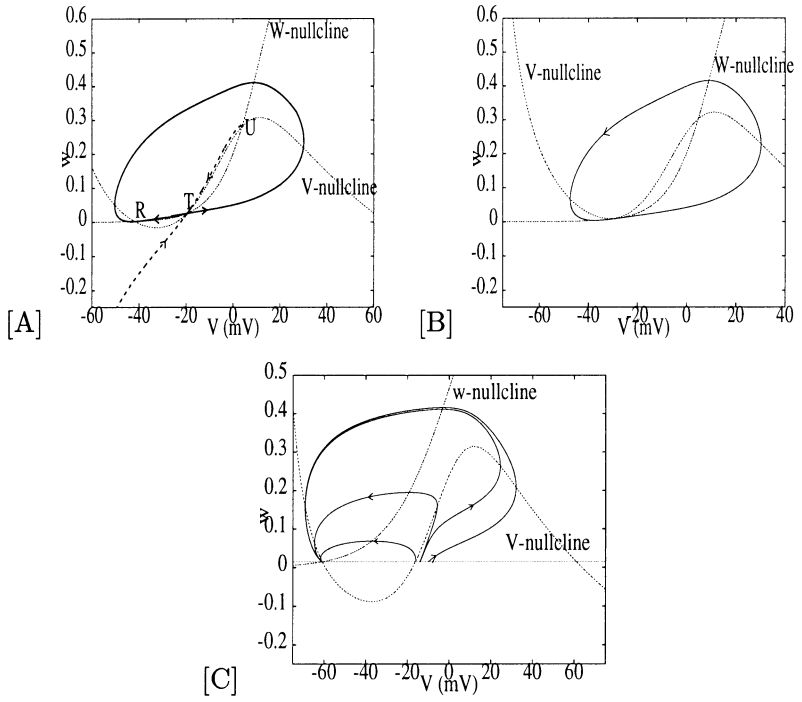

Figure 2: Phase plane for type I and type II neural membranes. Here we use the Morris-Lecar model as an example, with w being the activation variable and parameters set as in Rinzel and Ermentrout (1989). (a) Phase plane for a type I membrane in the excitable regime. Note that the stimulus-induced processions around the phase plane are of constant size and profile. Such processions r periodic solutions are said to live on an invariant circle. However, the rise time of spikes depends on stimulus amplitude. Here R is the attracting rest state, T is the saddle, and U is an unstable steady state. (b) Phase plane for type I membrane in oscillatory regime. Once again the spikes are of constant amplitude and live on the invariant circle. The voltage nullcline has been lifted by the added constant bias current. (c) Phase plane for type II membrane in the excitable regime. Note that the spikes are of variable amplitude.

θ-neuron. The parameters of the θ-neuron can be quantitatively related to physiologically observable quantities, and the dynamics reflect the nonlinear properties of the neuronal membrane.

We describe the neuron by a phase-variable θ. This phase represents the location of the voltage and activation state vector along the spike trajectory (see Figure 3a). The dynamics of the phase under noisy input are governed

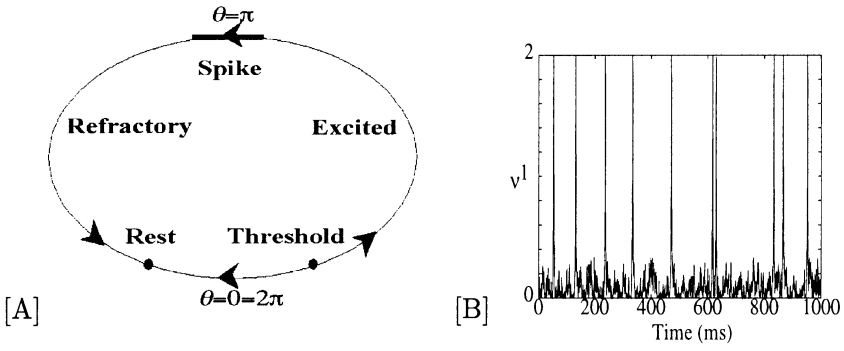

Figure 3: (a) Phase evolution on a circle and its analog in state of the membrane voltage. Note that the spike occupies a small region near π, and the model spends most of its time near the threshold. A suprathreshold stimulus pushes θ past the threshold and into the excited region. Here the regenerative dynamics that summarize active conductances carry the phase through the spike. (b) A representative spike train for the phase model excited by a random stimulus. Here we plot not θ but $v = 1 - \cos(\theta)$, which makes the spikes apparent.

by the following stochastic (Langevin) differential equation:

$$d\theta/d\tau = (1 - \cos\theta) + (1 + \cos\theta)(\beta + \sigma W_\tau) \qquad \theta \in [0, 2\pi], \tag{3.1}$$

for white noise input W_τ with intensity σ.[3] Here β is the bias parameter, which controls the excitability of the cell. The critical value is at $\beta = 0$. In the excitable regime, where β is negative, the model has an attracting rest state and a repelling threshold.[4]

In case of a subthreshold stimulus, the phase returns passively to rest, while a suprathreshold pulse causes the phase to rotate around the circle and produce a spike. In fact, if we plot the time evolution of $v = (1 - \cos(\theta))$ we can readily see the fast spike (see Fig. 3b).

3.1 Reduction to θ-Neuron. We present an outline of the mathematical reduction process, a more detailed description has been published in Ermentrout (1996b) and a complete mathematical treatment in Hoppensteadt and Izhkevich (1997).

The reduction relies on perturbation methods for the saddle-node bifurcation inherent in type I membranes. Heuristically we can describe the

[3] W_t is constructed by generating gaussian random deviates with variance proportional to $\sqrt{d\tau}$; the integral of W_t gives a Wiener process.

[4] These are given by $\theta_{rest} = -\arccos\frac{1+\beta}{1-\beta}$ and $\theta_{threshold} = \arccos\frac{1+\beta}{1-\beta}$, respectively.

behavior by a phase variable because the oscillations in the type I neuron are of invariant amplitude (i.e., the cell produces spikes of constant shape).

Let us consider a generic conductance model:

$$dV/dt = F_0(V) + \epsilon^2 N(V). \tag{3.2}$$

Here V is the vector of dynamical variables of the model (e.g., membrane voltage, activation variables), $F_0(V)$ is the nonlinear function that includes the membrane properties of the conductance model, and $N(V)$ is the input; ϵ is small. We assume that when $\epsilon = 0$, there exists an invariant circle around a single fixed point, which persists on both sides of the bifurcation. Then let the saddle node appear at the critical value V^*. We linearize $F_0(V)$ around that value and note that the Jacobian of $F_0(V)$ at V^* has a zero eigenvalue. Letting $V = V^* + \epsilon z\vec{e}$, where $\vec{e}$ is the eigenvector corresponding to the zero eigenvalue, the dynamics of equation 3.2 near the bifurcation are governed by

$$dz/dt = \epsilon(\eta + qz^2) + h.o.t., \tag{3.3}$$

which is the normal form for saddle-node dynamical systems. We now make a change of coordinates τ=ϵt and z=tan(θ / 2), and setting q to unity without loss of generality, we arrive at

$$d\theta/d\tau = (1 - \cos\theta) + \eta(1 + \cos\theta), \theta \in [0, 2\pi], \theta(0) = \theta(2\pi), \tag{3.4}$$

where η is proportional to the inputs in the original model.[5]

The reduction method determines how we can include a noise term to model the influence of a large number of positive and negative inputs of random strength arriving at random times. The additive input $N(V)$ in the full model (in equation 3.2) is reduced to η in the θ-neuron. Letting $\eta = (\beta + \sigma W_\tau)$ where β is the bias and W_τ models white noise, we arrive at the appropriate model for the random inputs. The o.d.e. for the phase in equation 3.4 then becomes the Langevin d.e.:

$$d\theta/d\tau = (1-\cos\theta) + (1+\cos\theta)(\beta+\sigma W_\tau), \theta \in [0,2\pi], \theta(0) = \theta(2\pi). \tag{3.5}$$

Note that this noise model is based solely on the mathematics of the reduction and reflects several important characteristics about how a neuron responds to inputs. The neuron is most sensitive to its inputs when at rest and most insensitive during the spike—when voltage is dominated by spike-generating currents—and the refractory periods that follow. The inputs in the θ-neuron are scaled by the $(1 + \cos(\theta))$ and have the most effect on the

[5] In general, η and q can depend on time and phase and can be calculated directly from the original neural model; see Ermentrout (1996b).

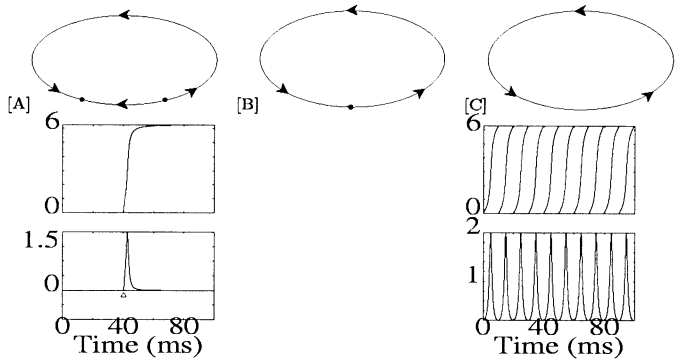

Figure 4: Saddle-node dynamics on an invariant circle. The upper trace shows the location of critical points on the invariant circle, the middle trace shows the behavior of the phase variable, and the lower trace is the trace of $(1 - \cos(\theta))$ showing the spikes. The horizontal axis in the lower two traces gives time in ms. (a) Excitable regime with $\beta = -0.3$, the spike is evoked by a suprathreshold pulse stimulus marked by the triangle. (b) Bifurcation with saddle-node point, $\beta = 0$. The homoclinic trajectory (one that joins a critical point to itself) has an infinite period. (c) Oscillatory regime with $\beta = 0.3$. Autonomous periodic processions in the phase variable and spikes in $(1 - \cos(\theta))$ are present.

phase θ when the cell is close to the resting potential, and little or no effect when the cell is traversing through the spike. In this work, we present results for the white noise inputs, although similar arguments can lead to an appropriate model for Poisson-timed excitatory and inhibitory inputs.[6]

The deterministic behavior of the model has been described in detail in Ermentrout (1996b). The main point is that the θ-neuron reflects all the salient characteristics of the dynamics of the original full model. Since the θ-neuron is a canonical model for type I neural models, its dynamics reflect the saddle-node-based spike-generating behavior of any type I neural model, including the spike latency sensitivity to stimulus amplitude. The θ-neuron exhibits both excitable and tonically oscillating regimes, depending on the bias β. Figure 4 summarizes the behavior of the model for different bias values.

[6] $\eta = (\beta + g_e dN_{ex} + g_i dN_{in})$, where dN_{ex} dN_{in} are unit events with arrival times given by Poisson processes with intensity λ_{ex} and λ_{in}, respectively. The amplitudes of ESPSs and IPSPs are given by g_{ex} and g_{in}. We should note that the bias + white noise input model would not work in the limit of low EPSP amplitudes, long EPSP duration, and high arrival rates where the net effect would be a mean DC current. However, for this work, we start by assuming that the inputs to the soma carry a significant degree of variability.

4 Results of Numerical Experiments for θ-Neuron

To study the stochastic dynamics of model 3.1, we carried out numerical simulations using the XPPAUT differential equation exploration package (Ermentrout, 1996a) The equations were integrated on a circle with period of 2π using a stochastic version of the Euler method with time step of 0.05 ms. The noise was generated by XPP using standard algorithm for construction of Wiener process (see footnote 3 and Kloeden & Platen, 1994). The voltage time series was converted into spike-train data for which we computed ISI CVs and histograms. The interspike interval (ISI) data were examined to ensure stationarity.

4.1 The Excitable Regime: Noise-Induced High-CV Firing. In the excitable regime (β below 0), firing is induced purely by the noise inputs. ISI histograms of the noise-driven excitable θ-neuron show a characteristic peak. That is, for a given β, the noise induces a characteristic mean ISI. The mean ISI is controlled by both the constant bias and the amplitude of the noise process. As the β becomes more positive or σ increases, the peak in the ISI histogram moves to the left (see Figures 5a and b) increasing the mean firing rate. The noise and bias have similar effects on the firing rate. However, they have differential effects on the ISI variability.

Increasing the amplitude of the noise inputs while holding the bias constant has comparatively little effect on the scale of the ISI histogram. For $\beta = -0.3$, the high-noise histogram has qualitatively equal mass in the tail as the low-noise one (see Figure 5a). Consequently, when the firing rate is controlled by the noise intensity, the CV remains high and does so across a wide range of mean ISIs, with a slight downward trend toward the shorter ISIs (see Figure 6c).

We propose the following explanation. With a constant negative bias, the distance to the threshold and the region where the motion is slow are held constant. The firing rate then depends on the mean frequency of random crossings of the threshold. Because of the spike latency characteristics of type I membranes, the variance of the ISIs depends on the threshold crossings, and also on the amplitudes of the suprathreshold inputs. As the variance of the noise input goes up, the variability in the amplitude of the suprathreshold shocks increases, thereby driving the variability of the spike latencies up. Thus, the CV remains largely invariant for a wide range of firing rates. As the firing rate becomes very large, the refractory period exerts a regularizing influence, and the CV begins to decrease.

On the other hand, when we hold the noise amplitude fixed, increasing β gives spike trains with lower CVs and ISI histograms with progressively shorter tails (see Figure 5b). We suggest that this happens because as the rest and threshold approach each other, the active spike currents (here intrinsic regenerative behavior of the phase) are much easier to activate. These currents then drown out the variability in the inputs. To put it another way, the

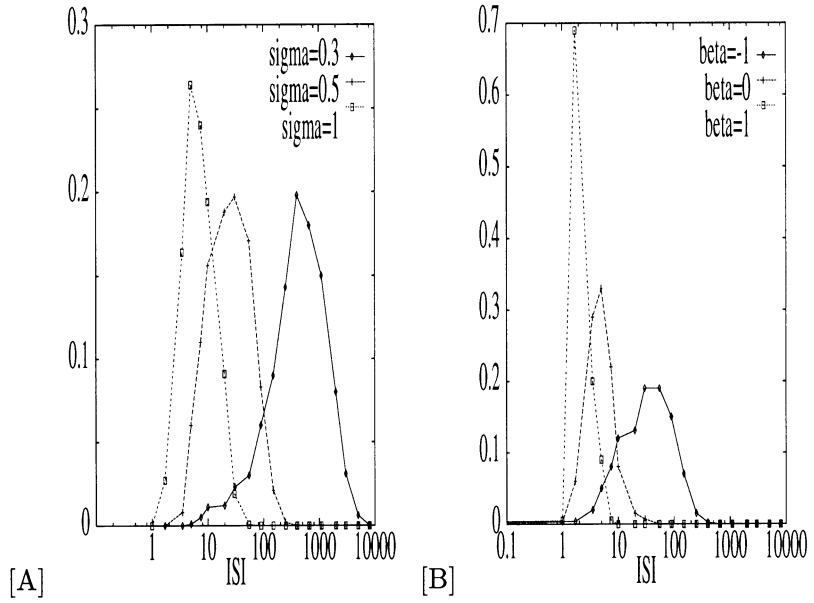

Figure 5: Normalized histograms for θ-neuron, ISIs plotted on log scale. (a) $\beta = -0.3$ and noise amplitude varied. Note that the left tail of the histogram appears to shorten as σ increases; partially due to the log scale and also because with higher input variance, the mode moves to closer to the smallest possible ISI. (b) Noise amplitude $= 1$ and β varied. The mean ISI of deterministic oscillations for $\beta = 1$ case is 3.14 ms.

more excitable cell is much less dominated by the slow dynamics near the rest state, and the range of inputs that would cause highly variable spike is decreased.

4.2 The Oscillatory Regime: Noise-Modulated Periodic Firing. At supercritical bias values (β above 0), the model fires periodically even without the noisy inputs. In this regime, the noise modulates the mean frequency of firing, while the firing is comparatively regular with low CVs and short-tailed ISI histograms. Once again our explanation holds. The dynamics of the oscillating cell are dominated by the active currents, and the noise inputs exert a comparatively weak influence on the firing behavior.

5 Numerical Simulation of Stochastic Morris-Lecar

To corroborate our findings in the θ-neuron, we studied the M-L model. The M-L has the advantage of being a conductance-based model that can be put

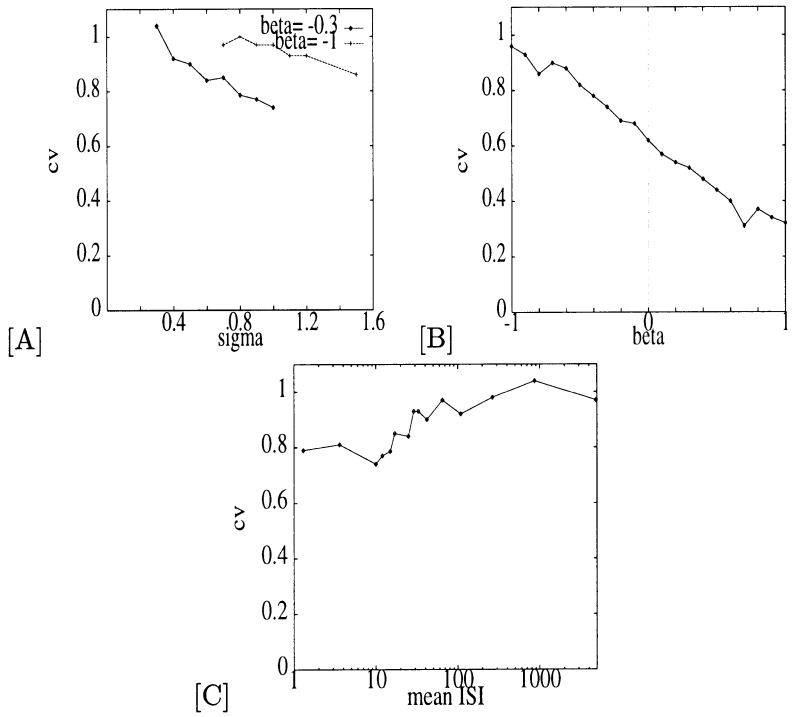

Figure 6: CV results for θ-model. (a) CV remains high across a wide range of noise parameters. (b) CV decreases linearly with β. (c) CV remains high across a wide range of firing rates, when such are controlled by noise. Here $\beta = -1$, σ varied.

into both type I and type II regimes depending on the chosen parameters. We examined the hypothesis that for equivalent excitability, the type I model yields high CVs under a variety of random input conditions, while the type II model gives a regular firing pattern. For our simulations, both type I and type II models were parameterized by the deviation from the critical input bias current, $(I_{bias} - I_{critical})$, to fix the excitability conditions.[7] Equations and exact parameter values for both models are given in the appendix. For both models, the negative deviation indicates the excitable regime, while the positive corresponds to an intrinsic oscillator. The inputs consist of instantaneous excitatory and inhibitory postsynaptic currents (EPSCs and IPSCs, respectively) with Poisson-distributed arrival times. The amplitudes of EP-

[7] For type I Morris-Lecar $I_{critical} = 40$ mV, type II, $I_{critical} = 100$ mV.

SCs were set to ensure integration of many inputs to generate a spike. Both inputs were modeled as simple exponentials with time constants of 1 ms. The IPSC arrival rate for all simulations was kept constant, while the rate of EPSCs was varied.[8] The random arrival times were generated by using two-state Markov chains with transition probabilities set to give Poisson arrival proccesses for inhibition and excitation with desired means (this feature is built into XPP).

5.1 Morris-Lecar in Type I Regime. Type I Morris-Lecar shows high CV behavior. The type I model yields a wide range of firing rates for different excitability and input parameters. There is a strong dependence of the CV on the excitability of the cell (see Figure 7, upper trace). In the excitable regime, CV values close to unity are observed, with the CV clearly decreasing as the model passes into the oscillatory regime, yet the CV is always above 0.3. In the oscillatory regime, the inputs are dominated by the intrinsic dynamics of the oscillating membrane, and the mean ISI reflects the intrinsic frequency of oscillation. On the other hand, for a model in the excitable regime, the CV value is comparatively insensitive to the rate of arrivals of EPSPs. Consequently the CV remains consistently high for a wide range of firing rates when these are controlled by the variability of inputs. Also the CVs for type I spike train for the M-L model are largely independent of the inhibition-to-excitation ratio.

5.2 Morris-Lecar in Type II Regime. We now modify the M-L model to reflect type II excitability. Compared to type I, this model in the excitable regime exhibits a narrow range of ISIs, which are in fact close to the frequency of oscillations at criticality. The CV is not sensitive to the bias current (see Figure 7, lower trace) and at no value of EPSP rate does the model exhibit CVs above 0.5. In fact, the only way to achieve high CV value for this model is to resize the amplitude of EPSP to make the threshold near to one event, with the model doing no integration.

6 Summary

In this work we asked whether dynamics of spike generation consistent with cortical neuron data can account for the statistics of cortical spike trains. Using a canonical model, we show that type I cells driven to firing by the noisy inputs give highly variable spike trains. On the other hand, intrinsic oscillators have a much more regular spiking behavior. Furthermore, type I M-L results clearly show high CV levels, with excitation dominating the random inputs, while type II models give regular firing. Our results are

[8] The ratio of inhibition to excitation as defined in Troyer and Miller (1997) $R = (g_i|V - V_i| * rate_i)/g_e|V - V_e| * rate_e)$ varied from 0.1 to 2.

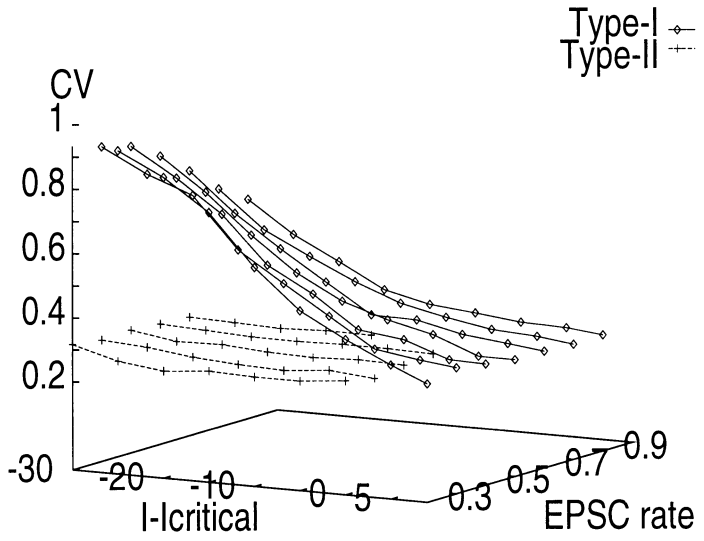

Figure 7: CV results for Morris-Lecar models. The upper trace shows type I behavior, and the lower trace is type II. Note that IPSC rate was 0.3 for all simulations. EPSC rate varied.

in contrast to the suggestions by Softky and Koch (1993), who imply rather specific synaptic organization of inputs and restrictive parameter regime for the dendritic spikes, or to the Bell et al. model (1995), which requires not only a balance of inhibitory and excitatory inputs but also a very narrow subset of the parameter space. We are also able to reproduce neural variability without reliance on network dynamics. We provide a formal mathematical method to derive the θ-neuron from conductance-based models, and thus can give specific physiological meaning to the parameters.

High-CV spike trains are observed for the excitable θ-neuron and type I Morris-Lecar. The saddle-node bifurcation characteristic of such membranes underlies the observed results. In particular, we suspect that the CVs are high because the noise randomly "samples" large period orbits, leading to the spike latencies that are strongly dependent on the size of the time-dependent stimulus. Thus a stimulus that provides suprathreshold shocks of random amplitudes will evoke strongly variable ISIs for type I neurons.

In contrast are membranes with type II dynamics, where the oscillations arise with a nonzero frequency through a Hopf bifurcation. In such a system there are no long-period orbits for the noise to sample, and the spike latency for suprathreshold stimuli is bounded above. We observe generically low

CV values for the type II M-L even with inhibition and excitation balanced in the random inputs. We expect that type II neurons in general do not exhibit high CVs except under some very special conditions that ensure bistability (Bell et al., 1995).

We also observe that type I neurons that are driven to firing by random inputs exhibit high CV values generically, without the balance of excitation and inhibition. We suggest that the high "physiological gain" condition proposed by Troyer and Miller (1997) is a natural consequence of type I membrane dynamics. In fact, for type I models, gain is infinite near the threshold for onset of oscillations. The key, we suggest, is not the gain as such, but the range of input amplitudes that leads to significantly variant spike latencies. Furthermore, just like the "high"-gain IF neuron, type I models spend most of their time near a steady state and not depolarizing toward the threshold. Essentially the dynamics of the saddle-node-induced firing imply a highly nonuniform motion for the voltage-activation trajectory with very slow motion near the rest state.[9] Then the cell spends most of its time near the rest and is pushed to firing by the fast swings in the input current. In this way, the spike-generating mechanism acts as a de facto high-pass filter. It is particularly interesting to note that Hodgkin in his 1948 paper observed that type I spikers (axons in his case) produced a much more variable firing pattern than the type II spikers. Arbitrary spike delay latencies were also reported in the same work.

At the same time θ-neuron and the M-L are not coincidence detectors in the sense that both code the mean input rate with a mean output rate. This means that high CVs cannot be used as a litmus test to solve the rate versus coincident coding dilemma. However, the delay to spike characteristics of type I neurons suggests that cortical neurons can act as amplitude to spike latency converters, and perhaps pass information about the temporal structure of the stimulus not only in the firing rate but also in the relative timing of individual spikes. In this way, the spike train as a whole would look very noisy, yet the information about the stimulus would be encoded quite precisely by the timing of spikes. In order for this coding mechanism to work, the cells must respond robustly to aperiodic inputs, and in fact data from Mainen and Sejnowski (1995) show highly reproducible responses to repeated noiselike stimuli in vitro. Robust spike timing despite noisy firing was also recently reported by Reich et al. (1997) in visually stimulated in vivo cat retinal ganglion cells and lateral geniculate nucleus for high-contrast stimuli, while low-contrast stimuli seemed to lead to less

[9] Such "slowdown" near the rest can result in a real neuron or biophysical model from a sodium current that is slow to activate at the beginning of the spike generation, with a steeply increasing voltage-dependent time constant. Alternatively, the same effect can be generated by an interaction of a slow potassium current that is partially activated at rest (e.g., I_m) and a fast sodium spike-generating current, or an inactivating potassium current (e.g., I_A).

robust responses. We found behavior similar to that reported in both reports above for the θ-neuron in our preliminary simulations. These results will be published elsewhere.

The θ-neuron model, like the integrate-and-fire model, is a one-dimensional caricature of a "real" neuron. Both models have arbitrarily low firing rates as the input current is lowered to the threshold. However, the way in which the frequency goes to zero is like $1/|\log(I - I^*)|$ in the integrate-and-fire model rather than the square root law that type I models and the θ-model obey. Similarly, the slope at criticality is infinite in both cases. The main difference lies in the latency to firing due to a suprathreshold stimulus. There is no notion of latency to firing in an integrate-and-fire model; either a stimulus is above threshold, in which case firing is instantaneous, or it is below threshold and no firing occurs. In the θ-model and in type I membranes, the latency is due to the saddle point. This enables cells to respond at arbitrarily long latencies after receiving a suprathreshold stimulus. This in fact was noted by Hodgkin (1948).

Our work suggests that cells with high CV spike trains are in the excitable regime as opposed to intrinsic oscillators. This may mean that cortical neurons are not intrinsic oscillators but are driven to firing by the inputs. Then coherent oscillations such as those observed in cortical networks depend critically on the presence and characteristics of the afferent and efferent inputs.

One interesting finding in this study is the dependence of CV on the excitability of the cells. The excitability in the simple models we present is set by the DC bias. In in vitro experiments, the bias current is the step current applied by the experimenter, but in in vivo neurons, any slow depolarizing or hyperpolarizing currents or effects of inputs impinging on distal dendrites and filtered by the dendritic tree can be viewed as bias currents. Some suggestions for changing bias currents include NMDA activation and muscarinic modulation of the M-current; then our work implies an interesting effect of slow modulation—that the slow modulatory synaptic currents can upregulate the spike rate by making the cell easier to fire and reducing accommodation, and also change the overall variability of the spike train. The effects of changing excitability on spike-train variability can be studied experimentally in pyramidal neurons by manipulating the slow modulatory currents (e.g., by applying NMDA agonists or muscarinic antagonists).

Finally, since our models become noisier as the input mean moves away from the repetitive firing threshold, the mechanism for generating highly noisy firing is not "balancing" of inhibition and excitation. As we have pointed out before, the key is the high-pass filtering property of the spike-generating mechanism when the spike is caused by a fast procession in the random input current. On the other hand, in the intrinsically oscillating cell, the inputs are dominated by the intrinsic currents that generate the periodic firing, with the random inputs having less influence on the statistics of the spike train. Thus, the further the cell is from being an intrinsic oscillator, the

more it is driven by the synaptic currents (relative to intrinsic currents) and the noisier is its output.

In summary, by focusing on the dynamics of the spike generation by a soma receiving random inputs, we propose that the dynamical mechanism of spike generation has a strong effect on the stochastic properties of neuronal activity. The dynamical mechanism in our work implies that spike generation in cortical pyramidal cells is consistent with saddle-node dynamics. This suggestion can be tested in in vitro experiments that examine spike latency curves and experimentally constructing phase response curves for cortical pyramidal neuron. In fact, we already know that arbitrarily low firing rates are observed experimentally. The saddle-node spike-generating dynamics can be caused by a number of biophysical mechanisms, and further experiments should be designed to pinpoint the precise combination of conductances that forms the substrate in a particular class of neurons.

Furthermore, we expect that cells that tonically oscillate (due to the slow depolarization) and are given noisy current input would not show high CVs. At the same time, experiments where a noisy current is injected into cells exhibiting type II dynamics should corroborate the idea that such spike-generating dynamics cannot produce high, irregular firing except for a rather specific parameter regime (e.g., where the cell is bistable).

Appendix: Morris-Lecar Equations

The Morris-Lecar equations that we used are based on the model that appeared in Rinzel and Ermentrout (1989). They have the form:

$$
\begin{aligned}
C\frac{dV}{dt} &= -g_{Ca}m_\infty(V)(V - V_{Ca}) - g_K w(V - V_K) - g_L(V - V_L) + I \\
\frac{dw}{dt} &= \phi(w_\infty(V) - w)/\tau_w(V) \\
m_\infty(V) &= .5(1 + \tanh((V - V_1)/V_2)) \\
w_\infty(V) &= .5(1 + \tanh((V - V_3)/V_4)) \\
\tau_w(V) &= 1/\cosh((V - V_3)/V_4))
\end{aligned}
$$

Standard values for type I membranes are $V_K = -80$ mV, $V_L = -60$ mV, $V_{Ca} = 120$ mV, $C = 20\ \mu\text{F}/\text{cm}^2$, $g_L = 2\ \mu\text{S}/\text{cm}^2$, $g_K = 8\ \mu\text{S}/\text{cm}^2$, $V_1 = -1.2$ mV, $V_2 = 18$ mV, $V_3 = 12$ mV, $V_4 = 17.4$ mV, $\phi = .067$, and $g_{Ca} = 4.0\ \mu\text{S}/\text{cm}^2$. For type II membrane simulations, parameters are the same except, $V_3 = 2$ mV, $V_4 = 30$ mV, $\phi = 0.04$, and $g_{Ca} = 4.4\ \mu\text{S}/\text{cm}^2$.

Acknowledgments

We thank Dr. Satish Iyengar and Dr. John Horn for fruitful discussions and Dr. Todd Troyer for valuable comments on earlier versions of this article. Work on this project was supported by NSF and NIMH.

References

Bell, A., Mainen, Z., Tsodyks, M., & Sejnowski, T. (1995). *"Balancing" of conductances may explain irregular cortical spiking* (Tech. Rep. No. INC-9502). San Diego: Institute for Neural Computation, University of California at San Diego.

Burns, B. D., & Webb, A. C. (1976). The spontaneous activity of neurons in the cat's visual cortex. *Proc. R. Soc. London (Biol.), 194*, 211–223.

Dean, A. (1981). The variability of discharge of simple cells in the cat striate cortex. *Exp. Brain Res., 44*, 437–440.

Ermentrout, G. B. (1996a). XPPAUT1.8—The differential equations tool. Available at www.pitt.edu/bardware.

Ermentrout G. B. (1996b). Type I membranes, phase resetting curves, and synchrony. *Neural Computation, 8*(5), 979–1001.

FitzHugh, R. (1961). Impulses and physiological states in models of nerve membrane. *Biophys. J., 1*, 445–466.

Hodgkin, A. L. (1948). The local changes associated with repetitive action in a non-medullated axon. *J. Physiol. (London), 107*, 165–181.

Hodgkin, A. L., & Huxley, A. F. (1952). A quantitative description of membrane current and its application to conduction and excitation in nerve. *J. Physiol. (London), 463*, 391–407.

Holt, G. R., Softky, W. R., Koch, K., & Douglas, R. J. (1996). A comparison of discharge variability in vitro and in vivo in cat visual cortex neurons. *J. Neurophysiol., 75*(5), 1806–1814.

Hoppensteadt, F. C., & Izhkevich, E. M. (1997). *Weakly connected neural networks*. New York: Springer-Verlag.

Kloeden, P. E., & Platen, E. (1994). *Numerical solutions to stochastic differential equations*. New York: Springer-Verlag.

Kroner, L., & Kaplan, E. (1993). Response variability in retinal ganglion cells in primates. *Proc. Natl. Acad. Sci., USA, 86*, 8128–8130.

Mainen, Z. F., & Sejnowski, T. J. (1995). Reliability of spike timing in neocortical neurons. *Science, 268*, 1503–1506.

McCormick, D. A., Connors, B. W., Lighthall, J. W., & Prince, D. A. (1985). Comparative electrophysiology of pyramidal and sparsely spiny stellate neurons of the neocortex. *J. Neurophysiol., 54*, 782–805.

Reich, D. S., Victor, J. D., Knight, B. W., Ozaki, T., & Kaplan, E. (1997). Response variability and timing precision of neuronal spike trains in vivo. *J. Neurophysiol., 77*, 2836–2841.

Ricciardi, L. M. (1994). Diffusion models of single neurons. In F. Ventriglia (Ed.), *Neural modeling and neural networks* (pp. 129–162). Oxford: Pergamon Press.

Rinzel, J., & Ermentrout, G. B. (1989). Analysis of neural excitability and oscillations. In K. Koch & I. Segev (Eds.), *Methods in neuronal modeling*. Cambridge, MA: MIT Press.

Shadlen, M. N., & Newsome, W. T. (1994). Noise, neural codes and cortical organization. *Curr. Op. Neurobiol., 4*, 569–579.

Smith, C. E. (1992). A heuristic approach to stochastic models of single neurons.

In T. McKenna, J. Davis, & S. Zornetzer (Eds.), *Single neuron computation* (pp. 561–588). San Diego: Academic Press.

Softky, W., & Koch, K. (1993). The highly irregular firing of cortical cells is inconsistent with temporal integration of random EPSPs. *J. Neurosci.*, *13*(1), 334–355.

Stein, R. B. (1965). A theoretical analysis of neuronal variability. *Biophys. J.*, *5*, 173–194.

Traub, R. D., & Miles, R. (1991). *Neuronal networks of the hippocampus.* New York: Cambridge University Press.

Troyer, T. W., & Miller, K. D. (1997). Physiological gain leads to high ISI variability in a simple model of a cortical regular spiking cell. *Neural Computation*, *9*(5), 971–985.

Usher, M., Stemmler, M., Koch, C., & Olami, Z. (1994). Network amplification of local fluctuations causes high spike rate variability, fractal firing patterns and oscillatory local field potentials. *Neural Computation*, *6*(5), 795–836.

van Vreeswijk, C., & Sompolinsky, H. (1996). Irregular spiking in cortex through inhibition / excitation balance. Poster presented at Computational Neural Systems Conference, Cambridge, MA.

Wilbur, W. J., & Rinzel, J. (1983). A theoretical basis for large coefficient of variation and bimodality in neuronal interspike interval distribution. *J. Theo. Biol.*, *105*, 345–368.

Wilson, M. A., & Bower, J. M. (1989). The simulation of large-scale neural networks. In K. Koch & I. Segev (Eds.), *Methods in neuronal modeling*. Cambridge, MA: MIT Press.

Received May 9, 1997; accepted November 14, 1997.